Research Article | Vol. 31, No. 21 / 9 Oct 2023 / Optics Express 35054
Optics EXPRESS

Design method for a small F-number two-material uniform dispersion immersion grating imaging spectrometer

YANG LIU,[1,2] JINHUAN LI,[3] PENGFEI ZHANG,[3] AIMING ZHOU,[3] XIAOXU WANG,[1,*] JUNBO WANG,[4,5] BO LI,[1] GUANYU LIN,[1,6] GUOCHAO GU,[1] AND HANSHUANG LI[1]

[1]*Changchun Institute of Optics, Fine Mechanics and Physics, Chinese Academy of Sciences, Changchun 130033, China*
[2]*University of Chinese Academy of Sciences, Beijing 100049, China*
[3]*Shanghai of Institute of Satellite Engineering, Shanghai 200240, China*
[4]*Changchun College Of Electronic Technology, Changchun 130000, China*
[5]*College of Optoelectronics Science, Changchun 130000, China*
[6]*Innovation Center for FengYun Meteorological Satellite, Beijing 100081, China*
[*]*wxxzxcxxx@qq.com*

Abstract: Immersion gratings have high dispersion efficiency and have important application value in miniaturized imaging spectrometers, but its serious dispersion nonlinearity causes difficulties in calibration and image processing, which limits its application range. To solve this, this paper presents a design method for a two-material linear dispersion immersion grating device design method, and a compact small F-number immersion grating spectrometer based on it. First the vector form dispersion equation of the two-material immersion grating is derived and the linear spectral dispersion immersion grating design process is given, then a compact small F-number uniform dispersion imaging spectrometer is given as a design example using the proposed method. The results show that when the operating band of the system is 1590-1675 nm, the spectral resolution is better than 0.25 nm, and F-number can achieve better than 2. Compared with traditional single-material immersion grating imaging spectrometer, the designed imaging spectrometer dispersion linearity is significantly improved. Finally, the influence of prism materials, structure parameters and grating parameters on dispersion nonlinearity is analyzed. Design and analysis results show that the proposed two-material immersion grating device has much better spectral dispersion nonlinearity correction ability, and its design method can provide reference to the compact spectrometer design based on immersion gratings.

1. Introduction

Imaging spectrometer is a kind of instrument combining spectroscopy and imaging, which can obtain two-dimensional image information of target in space and spectral dimension at the same time. Since its rapid development in the 1980s, imaging spectroscopy has been widely used in atmospheric, ocean and land observations [1–9]. With the development of computational imaging technology, the requirement of imaging spectral system is further improved [10]. As the core component of spectrometer, grating directly determines the spectral resolution of the spectrometer. Immersion grating has higher spectral dispersion efficiency compared to common gratings, thus it has important application potential in compact imaging spectrometers. However, it also brings serious dispersion nonlinearity. increases the difficulty of spectral calibration and correction, and brings great difficulties for subsequent image processing [11–13], which severely limits its application field.

#502867 https://doi.org/10.1364/OE.502867
Journal © 2023 Received 10 Aug 2023; revised 31 Aug 2023; accepted 5 Sep 2023; published 3 Oct 2023

Optics EXPRESS

To correct the spectral dispersion nonlinearity of the prism and grating devices, many scholars have studied it in recent years. Fan et al. proposed to used Fery prisms to acquire uniformly dispersed Dyson imaging spectrometer. By analyzing the dispersion characteristics of two prisms of different materials, the achromatic prism group is selected, and the remaining aberrations are corrected by the toroidal reflector and lens group. The designed imaging spectrometer operates at 400-2500 nm, F-number is 3, spectral resolution is 10 nm, and has good dispersion linearity [14]. Liu Bing et al. established a mathematical model of a symmetrical prismatic combination splitter structure, analyzed the factors affecting its dispersion linearity, and finally obtained a coaxial imaging spectrometer with a working band of 400-1000 nm that met the requirements of linear dispersion, and its F-number was 5.55 [15]. Changsik Yoon et al. designed a free-form surface to achieve very low dispersion nonlinearity. The imaging spectrograph model was established for analysis The k nonlinearity is reduced from 2.47% to 2.79×10^{-5}% and 3.36×10^{-9}%, and the F-number of the system is greater than 6 [16]. In 1991, Vaarala et al. combined two dispersive elements, prism and grating, to obtain the prism-grating-prims(PGP) dispersion module, and developed the corresponding imaging spectrometer. Due to the different dispersion characteristics of the prism and the grating, it has the ability to eliminate the the spectral smile and the nonlinearity of dispersion to a certain extent. However, Vaarala et al. did not derive this in detail, so as to obtain the best correction effect for the initial structure of PGP module [17]. On this basis, Xuan Zhang et al. studied a direct view spectrometer using PPG as the light dispersive element. Its operating band is 400-990 nm, spectral resolution is 1.5 nm, and it has the characteristics of uniform dispersion. However, the system uses multiple planar mirrors to realize the design of direct vision, which is relatively difficult to install and adjust, and its F-number is greater than 6, the light collecting ability is weak, and the signal-to-noise ratio is low [18].

High diffraction order immersion gratings can achieve high spectral resolution while greatly reducing the volume and weight of the system. However, there is a lack of relevant literature on the correction of its spectral dispersion nonlinearity. In addition, due to the need for higher light-collecting capacity and signal-to-noise ratio of the instrument, the system needs to have a smaller F-number. Light and miniaturization is also the focus of current research [19,20]. In order to solve the above problems, based on the dispersion difference between different materials, a design method of linear dispersion immersion grating, and a small F-number hyperspectral imaging spectrometer using the proposed two material immersion grating as dispersion module is proposed in this paper. By establishing the model of dispersion device, the initial structure of the system is derived, and the structural parameters of the system are further optimized to achieve high imaging quality and nonlinear dispersion correction. Finally the sensitivity of the two material immersion grating device on the spectral dispersion linearity is discussed.

2. Theoretical analysis

2.1. Theory of traditional single material immersion grating

Figure 1 shows the schematic diagram of the traditional single-material immersion grating. Light incident by air reaches the surface of the medium, and after refraction through the surface, diffraction occurs at the grating surface, and the diffracted light refracts through the surface again. In order to analyze the dispersion uniformity of the dispersion module, the dispersion expression is derived, β is the vertex angle, n is the refractive index of the material.

According to the law of refraction:

$$n_0 sini_a = nsini'_a. \tag{1}$$

According to the geometric relationship, the grating incidence angle is:

$$i_b = \beta + i'_a. \tag{2}$$

Optics EXPRESS

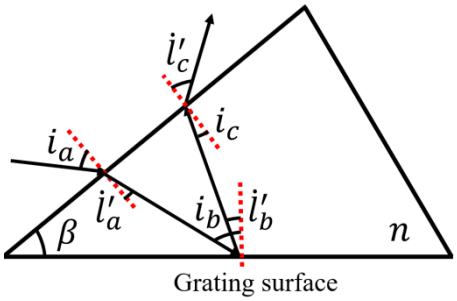

Fig. 1. Schematic diagram of single-material immersion grating.

According to the grating equation:

$$n(sini_b + sini'_b) = Nm\lambda. \tag{3}$$

And:

$$i_c = \beta - i'_b. \tag{4}$$

The final dispersion angle is:

$$i'_c = arcsin\left(\frac{n}{n_0}sini_c\right). \tag{5}$$

By differentiating the wavelength, the dispersion equation of the traditional immersed grating can be obtained:

$$\frac{di'_c}{d\lambda} = \frac{\frac{sini_c}{n_0}\frac{dn}{d\lambda} + \frac{n_1}{n_0}cosi_c\frac{di_c}{d\lambda}}{\sqrt{1-\left(\frac{n_1}{n_0}sini_c\right)^2}}. \tag{6}$$

The dispersion equation represents the change of diffraction angle with wavelength. When the dispersion equation is constant, it can be considered that the diffraction angle does not change with wavelength, and the system has the characteristics of uniform dispersion. In the formula $dn/d\lambda$ can be obtained from Sellmeier's empirical formula, and the coefficients of glass refractive index for B_1, B_2, B_3, C_1, C_2 and C_3 can be obtained by searching the glass database.

$$\frac{\mathrm{d}n}{d\lambda} = \frac{\left[\frac{B_1C_1\lambda}{(\lambda^2-C_1)^2} + \frac{B_2C_2\lambda}{(\lambda^2-C_2)^2} + \frac{B_3C_3\lambda}{(\lambda^2-C_3)^2}\right]}{\sqrt{1+\frac{B_1\lambda^2}{\lambda^2-C_1} + \frac{B_2\lambda^2}{\lambda^2-C_2} + \frac{B_3\lambda^2}{\lambda^2-C_3}}} \tag{7}$$

When the system is uniformly dispersed, i'_c should satisfy the following formula, where A and B are both real numbers.

$$i'_c = A\lambda + B \tag{8}$$

From formula (7) we know that n contains λ^2. In the dispersion module, the dispersion angle i'_c is not zero, and it can be seen from formula (1) to formula (5) that i'_c cannot satisfy formula (8). To sum up, it is difficult to achieve completely uniform dispersion theoretically when the traditional immersion grating of a single material is used as the dispersion module. On this basis, we discuss the immersion grating composed of two materials, derive its dispersion formula, and verify its rationality. It will greatly improve the dispersion uniformity of the immersion grating and reduce its influence on the subsequent data processing.

Optics EXPRESS

2.2. Theory of double material immersion grating

Dispersion module is the core part of the spectrometer system, which has the function of dispersing the beam. Based on the different dispersion characteristics of different materials, the two-material immersion grating is used to correct the dispersion nonlinearity of the system. To establish the vector dispersion equations related to beam angle, deflection angle between materials, deflection angle of grating surface, grating parameters and materials. Through theoretical calculation, the parameters satisfying the uniform dispersion condition and system index are found, and the initial structure of the spectral module is finally determined by iterative algorithm.

As shown in Fig. 2, Figure (a) is the meridian section of the dispersion module, and Figure (b) is the sagittal section of the dispersion module. The refractive index of air is n_0, the refractive index of the first material is n_1, and the refractive index of the second material is n_2. The deflection angle of the interface between the two materials is α, and the deflection angle of the grating surface is β. In order to analyze the dispersion uniformity of the spectrometer, it is necessary to derive the dispersion expression of the immersed grating module. Let $\overrightarrow{P_n}$ be the unit normal vector of the interface of each medium, and $\overrightarrow{R_n}$ be the unit vector of light in each medium.

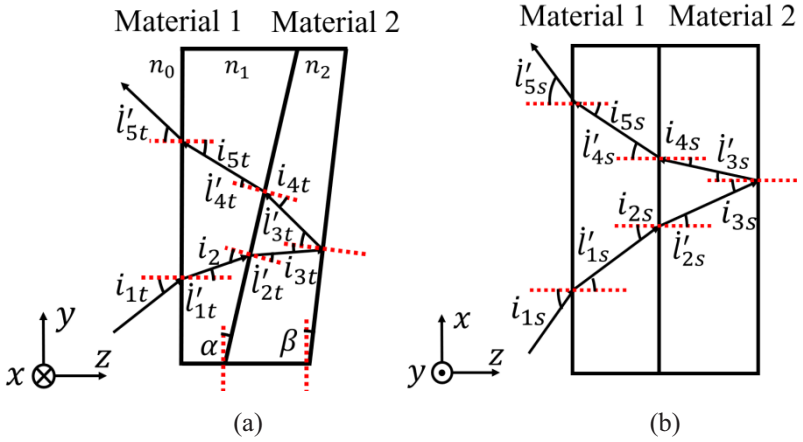

Fig. 2. Schematic diagram of two-material immersion grating.

2.2.1. Vector form of the refraction law

The known vector form of the refraction law [21], where n and n′ are the refractive indices of the medium in which the incident light and the refracted light are located, respectively. $\vec{P}$ is the unit normal vector of the interface. $\overrightarrow{R_0}$ is the unit vector of incident light, $\overrightarrow{R'_0}$ is the unit vector of refracted light.

$$n'\overrightarrow{R'_0} - \vec{P}(n'\overrightarrow{R'_0} \cdot \vec{P}) = n\overrightarrow{R_0} - \vec{P}(n\overrightarrow{R_0} \cdot \vec{P}) \tag{9}$$

In order to facilitate subsequent derivation, it is reduced to an angle-dependent form. According to the mathematical formula can be obtained:

$$\overrightarrow{R'_0} \cdot \vec{P} = cosi' \tag{10}$$

$$\overrightarrow{R_0} \cdot \vec{P} = cosi. \tag{11}$$

Where i is the incidence angle and i' is the refraction angle.

Finally, the vector form of the refraction law is:

$$n'\overrightarrow{R'_0} - n\overrightarrow{R_0} = (n'cosi' - ncosi)\vec{P}. \tag{12}$$

Optics EXPRESS

2.2.2. Vector form of diffracted light

When the incident light has off-axis angle in tangential and saggital orientations, the incident light, diffracted light and the normal lines of the grating are no longer coplanar [22]. As shown in Fig. 3, the coordinate system is established with the normal of the grating plane as the z-axis, $\overrightarrow{R_G}$ and $\overrightarrow{R'_G}$ are the unit vectors of incident light and diffracted light, respectively. Angle θ is the angle between the diffracted light $\overrightarrow{R_G}$ and the z-axis, and angle φ is the angle between the projection vector of the diffracted light $\overrightarrow{R_G}$ on the xy plane and the x-axis. Angle θ' is the angle between the diffracted light $\overrightarrow{R'_G}$ and the z-axis, and angle φ' is the angle between the projection vector of the diffracted light $\overrightarrow{R'_G}$ on the xy plane and the x-axis. The known vector form of grating equation [23]:

$$nsin\theta' cos\varphi' = sin\theta cos\varphi + Nm\lambda \tag{13}$$

$$nsin\theta' sin\varphi' = sin\theta cos\varphi. \tag{14}$$

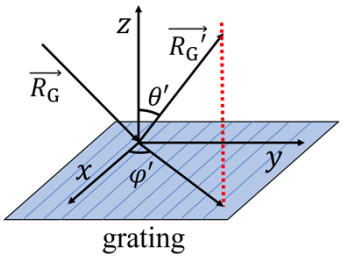

Fig. 3. Optical path diagram of grating surface.

The above equations can be solved to obtain the diffraction angle θ' and the diffraction azimuth angle φ':

$$\theta' = arcsin\frac{1}{n}\sqrt{sin^2\theta sin^2\varphi + (sin\theta cos\varphi + Nm\lambda)^2} \tag{15}$$

$$\varphi' = arctan\frac{sin\theta cos\varphi}{sin\theta cos\varphi + Nm\lambda}\ . \tag{16}$$

Where N is the number of lines per millimeter of grating, m is the diffraction order, and λ is the wavelength. According to the geometric relation, it can be deduced that the diffracted light $\overrightarrow{R'_G}$ with the grating plane normal as the z-axis is:

$$\overrightarrow{R'_G} = (sin\theta' cos\varphi', sin\theta' sin\varphi', cos\theta'). \tag{17}$$

2.2.3. Dispersion uniformity of optical systems

As shown in the Fig. 2, according to the basic geometric relationship, obtained:

$$\overrightarrow{R_1} = (sini_{s1}, sini_{t1}, cosi_{t1}) \tag{18}$$

$$\overrightarrow{P_1} = (0, 0, 1). \tag{19}$$

The incidence angle of surface 1 is:

$$i_1 = arccos(\overrightarrow{R_1} \cdot \overrightarrow{P_1})\ . \tag{20}$$

Optics EXPRESS

According to the refraction law of light, the refraction angle of surface 1 is:

$$i_1' = arcsin\left(\frac{n_0}{n_1} sini_1\right). \tag{21}$$

According to the refraction law of vector form, it is obtained:

$$n_1\overrightarrow{R_2} - n_0\overrightarrow{R_1} = (n_1 cosi_1' - n_0 cosi_1)\overrightarrow{P_1} \tag{22}$$

and then:

$$\overrightarrow{R_2} = \frac{n_0\overrightarrow{R_1} + (n_1 cosi_1' - n_0 cosi_1)\overrightarrow{P_1}}{n_1} . \tag{23}$$

Given that the deflection angle of interface 1 is α, can be obtained:

$$\overrightarrow{P_2} = (0, -sin\alpha, cos\alpha). \tag{24}$$

The same can be obtained:

$$i_2 = arccos(\overrightarrow{R_2} \cdot \overrightarrow{P_2}) \tag{25}$$

$$i_2' = arcsin\left(\frac{n_1}{n_2} sini_2\right) \tag{26}$$

$$\overrightarrow{R_3} = \frac{n_1\overrightarrow{R_2} + (n_2 cosi_2' - n_1 cosi_2)\overrightarrow{P_2}}{n_2} . \tag{27}$$

Given that the deflection angle of the grating surface is β, can be obtained:

$$\overrightarrow{P_3} = (0, -sin\beta, cos\beta) \tag{28}$$

$$i_3 = arccos(\overrightarrow{R_3} \cdot \overrightarrow{P_3}) . \tag{29}$$

According to the grating equation in vector form, the diffraction angle of the grating surface is obtained:

$$i_3' = arcsin\frac{1}{n_2}\sqrt{sin^2 i_3 sin^2\varphi + (sini_3 cos\varphi + Nm\lambda)^2} . \tag{30}$$

Since the grating has a deflection of β angle, and according to 2.2.2, we can get $\overrightarrow{R_4}$:

$$\begin{aligned}\overrightarrow{R_4} = (&sini_3' cosi_{3xy}', sini_3' sini_{3xy}' cos\beta - cosi_3' sin\beta,\\ &sini_3' sini_{3xy}' sin\beta + cosi_3' cos\beta)\end{aligned} . \tag{31}$$

And then:

$$\overrightarrow{R_5} = \frac{n_2\overrightarrow{R_4} + (n_1 cosi_4' - n_2 cosi_4)(-\overrightarrow{P_2})}{n_1} \tag{32}$$

$$i_5 = arccos[\overrightarrow{R_5} \cdot (-\overrightarrow{P_1})] . \tag{33}$$

Finally, the overall dispersion angle of the two-material immersion grating module is obtained:

$$i_5' = arcsin\left(\frac{n_1}{n_0} sini_5\right) . \tag{34}$$

The dispersion equation is obtained by differentiating it with respect to wavelength:

$$\frac{di_5'}{d\lambda} = \frac{\frac{sini_5}{n_0}\frac{dn_1}{d\lambda} + \frac{n_1}{n_0} cosi_5 \frac{di_5}{d\lambda}}{1 - \left(\frac{n_1}{n_0} sini_5\right)^2} . \tag{35}$$

Where $dn_i/\ d\lambda$ can be obtained by Sellmeier's empirical formula, and the central wavelength incidence angle i_1 is determined by the front lens group.

Optics EXPRESS

From the above analysis, it can be seen that using the double-material immersion grating as the dispersion element can theoretically achieve more uniform dispersion, and the dispersion module parameter combination is not unique. Therefore, the grating parameters can be determined according to the spectral resolution and other indicators, and the material can be selected initially, and then the corresponding structural parameters can be calculated according to the dispersion formula. Multiple sets of results are obtained repeatedly, unreasonable structures are eliminated, and finally the dispersion module parameters are obtained.

2.3. Dispersion uniformity index evaluation

$|K_m - 1|$ was established as an evaluation index to evaluate the dispersion uniformity of the system. In the formula, λ_a, λ_b and λ_c represent three wavelengths respectively, and they have the relationship shown in formula (36). When the optical system is uniformly dispersed, the dispersion length between wavelength λ_a and wavelength λ_b on the image plane should be equal to the dispersion length between wavelength λ_b and wavelength λ_c. Therefore, the more uniform the dispersion, the closer the value of $|K_m - 1|$ is to 0.

$$\lambda_a - \lambda_b = \lambda_b - \lambda_c \tag{36}$$

$$K_m - 1 = (L_{\lambda_a} - L_{\lambda_b})/(L_{\lambda_b} - L_{\lambda_c}) - 1 \tag{37}$$

When the system dispersion is not uniform, the corresponding dispersion length of each band may not increase or decrease uniformly. Therefore, the dispersive nonlinearity with different characteristics may appear at long wave and short wave. To ensure that the system has uniform dispersion everywhere, We divide the band evenly and equally into n segments, denoted by λ_i, and i = 1,2,. . . n + 1. Where λ_1 represents the short wave at the edge, λ_{n+1} represents the long wave at the edge, and $\lambda_{(n+2)/2}$ represents the central wavelength. Three groups of wavelengths were selected and substituted into Eq. (37) to conduct a preliminary evaluation of the dispersion uniformity at short wave, long wave and the whole band. The first set of wavelengths are λ_1, $\lambda_{(n+2)/2}$ and λ_{n+1}, and $|K_1 - 1|$ is used to represent the evaluation index. The wavelengths of the second group are λ_1, λ_2 and λ_3, so that $|K_2 - 1|$ represents the evaluation index. The wavelengths of the third group are λ_{n-1}, λ_n and λ_{n+1}, so that $|K_3 - 1|$ represents the evaluation index.

2.4. Dispersion module design process

In the design of the small F-number uniform dispersion immersed grating hyperspectral imager, the structural parameters of the two-material immersed grating as the dispersion module are mainly designed. Its design flow is shown in Fig. 4.

1. According to the system's indicator requirements, the diffraction order m of the immersed grating, the number of lines per millimeter of grating N and the two materials of the immersed grating are initially selected.

2. According to the derived dispersion equation, combined with Sellmeier empirical formula. Two deflection angles α and β satisfying the condition of uniform dispersion are obtained.

3. The above structure is substituted into the initial module of the immersed grating to verify the rationality of the initial structure. Confirm the angle between the incident light and the diffracted light to prevent excessive lens size in subsequent lens sets. At the same time, it is necessary to pay attention to the value of deflection angle β, when the value is too large, it will cause the submerged grating module size is too large. If the system does not meet the requirements, return to Step (1) and start the calculation again.

4. $|K_m - 1|$ was used as the evaluation index to verify the dispersion uniformity of the whole system. If the system counters do not meet the requirements, return to Step (1) and start the calculation again.

Optics EXPRESS

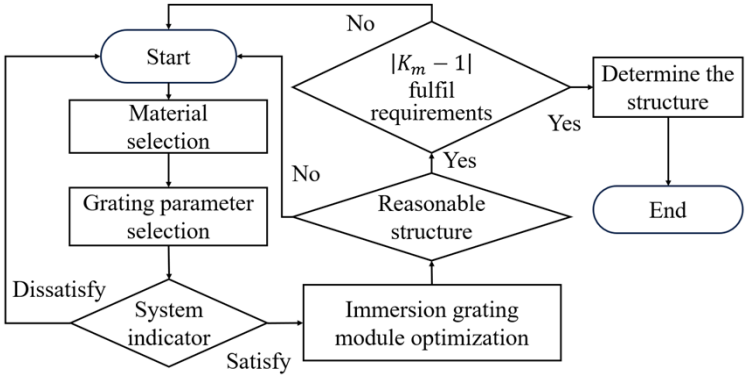

Fig. 4. Dispersion module design flow chart.

3. Design example

3.1. Optical layout

To demonstrate the performance of the proposed design method, we design an example of an imaging spectrometer using a two-material immersion grating as the dispersion element. As shown in Fig. 5. The whole is composed of the telescope system, the slit, the spectrometer system. The beam is incident by the telescope and imaged at the slit. In order to further separate the image plane from the slit, the outgoing light from the slit is deflected by a planar mirror. Then the reflected light is collimated by the lens group, and the collimated beam reaches the double-material immersion grating for dispersion. After the dispersion of the reflected light through the lens group again to achieve focus imaging, and finally reach the detector image plane.

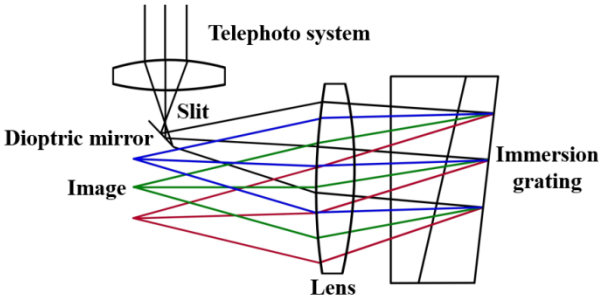

Fig. 5. Spectrometer system.

Immersion gratings can achieve high spectral resolution while greatly reducing the system volume. The immersion grating composed of two different materials is used as the dispersion element, and the dispersion nonlinearity of the system is corrected by the difference of the dispersion characteristics between the materials. At the same time, the design of small F-number has the advantages of enhancing the ability of light collection and improving the signal-to-noise ratio of the system. The collimation and focusing imaging of the beam can be achieved by using the lens group repeatedly, which can further reduce the volume of the system, and also facilitate the correction of the system aberration, so as to achieve high quality imaging while meeting the spectral resolution. In summary, the optical path design not only achieves uniform dispersion, but also has the advantages of small F-number, high spectral resolution, compact structure and so on.

Optics EXPRESS

3.2. System indexs

Optical system specifications are shown in Table 1. For the system, the autocollimation condition limits the structural parameters of the dispersion module, and it is difficult to achieve an ideal uniform dispersion. Therefore, if $|K_m - 1|$<0.003, the system has good dispersion uniformity. All evaluations were performed using the optical design software.

Table 1. Design index of imaging spectrometer

System Indexes	Value
Spectral Range/nm	1590-1675
F-number	2
Spectral resolution/nm	0.25
$\|K_m - 1\|$	< 0.003
MTF	>0.8@25lp/mm
Detector's pixel size/μm	10×10

3.3. Dispersion module parameter determination

Solar spectral irradiance contains information that characterizes the physical, chemical, thermal and dynamic characteristics of the solar atmosphere, and aerosol is one of the important influencing factors [24,25]. The operating band of the imaging spectrometer system is 1590-1675 nm, and the spectral resolution is 0.25 nm, which can effectively detect aerosols and trace gases in the atmosphere. When evaluating the dispersion uniformity index, the working band is divided into 8 equal bands, that is, n = 9. In addition, F-number is chosen as 2 to achieve stronger light-gathering ability and higher signal-to-noise ratio of the system.

For the immersed grating dispersion module, the grating diffraction order k = 4 and the grating engraving line 301lp/mm are selected. Material 1 is HZF88 from Chengdu Guangming Glass Library, and material 2 is SILICA, one of the commonly used materials for immersion grating. After iterative optimization, it is determined that the deflection angle α between material 1 and material 2 is 37.357°, and the deflection angle β of the grating surface is 25.998°.

3.4. Design example

The system band was set to 1590-1675 nm, the overall system variable ratio was 1, and the image square F-number of the designed telescope was 2. The lens group structure has higher degrees of freedom to achieve higher imaging quality. The partial collimation system of the spectrometer and the focusing imaging system use the same set of lenses, which can avoid the phenomenon of beam compression caused by the excessive diffraction angle of the grating. After the parameters of the immersion grating module are inserted into the software, the imaging quality of the system is improved by software optimization. And in order to reduce the cost, the system is designed with spherical lens.

Design using optical design software. Design the telescope in image space is the telecentric path. The spectrometer system in object space is the telecentric path. To facilitate the connection between the two systems. After docking the two systems, on the basis of ensuring that the independent imaging quality of the two systems meets the requirements of the index, the system is comprehensively optimized and fine-tuned to further improve the imaging quality of the whole system. Finally, the optical structure of the whole system is shown in Fig. 6. The spectral resolution of the system is better than 0.25 nm when the working band is 1590-1675 nm, and the F-number is 2. The volume of the system is less than $160 \times 120 \times 60 \text{mm}^3$, which has the characteristics of light miniaturization.

Optics EXPRESS

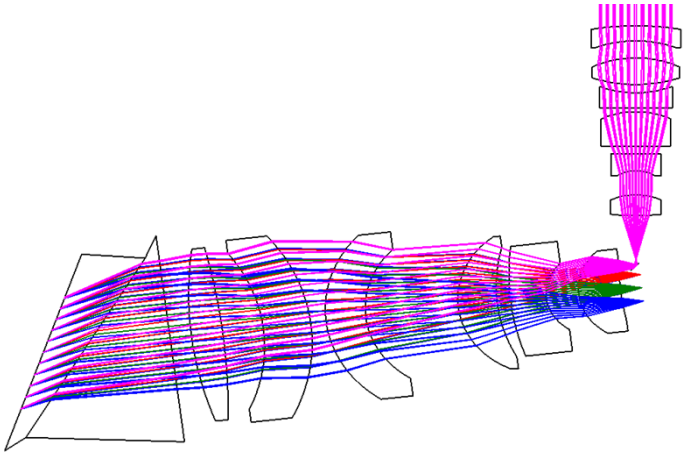

Fig. 6. Short-wave infrared small F-number uniform dispersion two-material immersion grating hyperspectral imaging spectrometer.

3.5. *Evaluation indicator*

3.5.1. MTF and spot diagram

MTF and spot diagram are one of the important indexes to evaluate the imaging quality of imaging spectrometer. As shown in Figs. 7 and 8, MTF is better than 0.83 at a cutoff frequency of 25lp/mm and an RMS radius of less than 7μm.

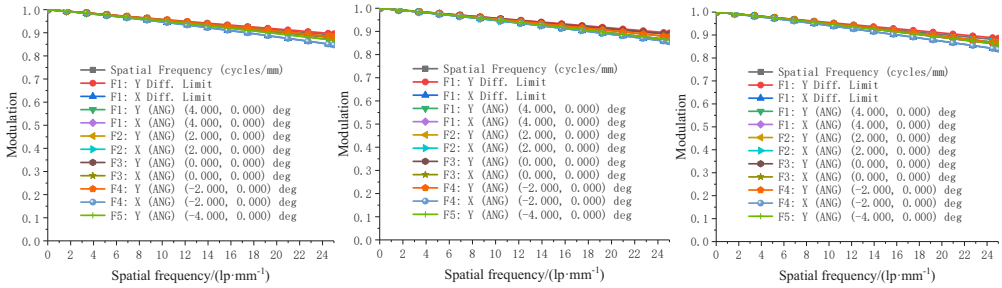

Fig. 7. MTF image at different wavelengths.

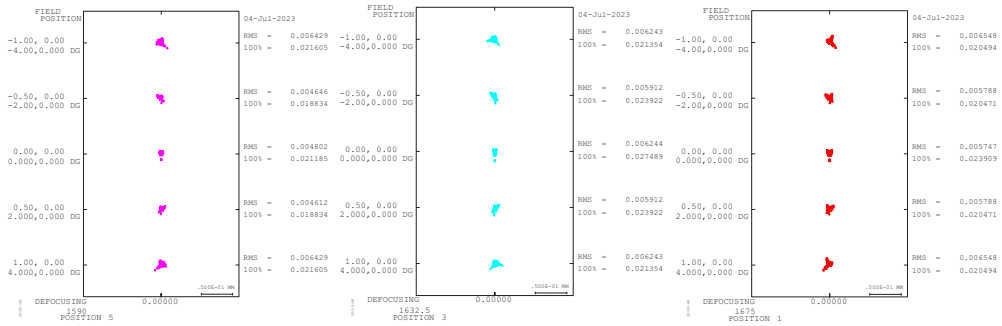

Fig. 8. RMS point diagrams at different wavelengths.

Optics EXPRESS

3.5.2. Dispersion uniformity

Also, optical design software is used to design a traditional single-material immersed grating imaging spectrometer with the same contents except the immersed grating material and deflection angle, and the same high imaging quality, for dispersion nonlinear comparison. After the wavelength of 1590-1675 nm is evenly divided into 8 segments, each wavelength length is 10.625 nm. List the corresponding dispersion lengths for each 10.625 nm. Every three adjacent wavelengths are substituted into Eq. (37) to obtain the dispersion uniformity index $|K_m - 1|$, and the closer the value is to zero, the more uniform the dispersion is. As shown in Fig. 9, the horizontal coordinate represents the wavelength, and the vertical coordinate represents the $|K_m - 1|$. The gentler the curve, the more uniform the dispersion. It can be seen that as a dispersion module, the double-material immersed grating has better dispersion uniformity than the conventional immersed grating imaging spectrometer. The index $|K_m - 1|$<0.0018 used to evaluate the dispersion linearity meets the requirement of less than 0.003.

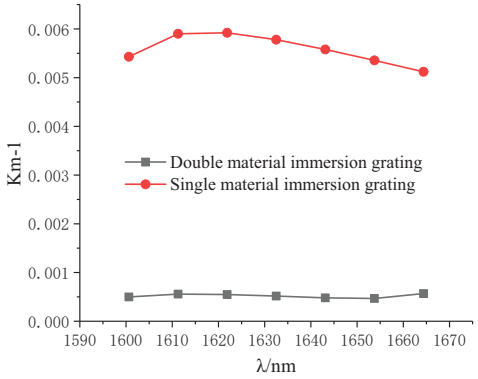

Fig. 9. Dispersion uniformity comparison diagram.

3.5.3. Spectral smile and keystone

As an important index to judge the imaging quality of the system, spectral smile and keystone are also the validation of the system design method, and the design results should also be checked. The spectral smile and keystone curves of the dual-material immersed grating imaging spectrometer are shown in Fig. 10.

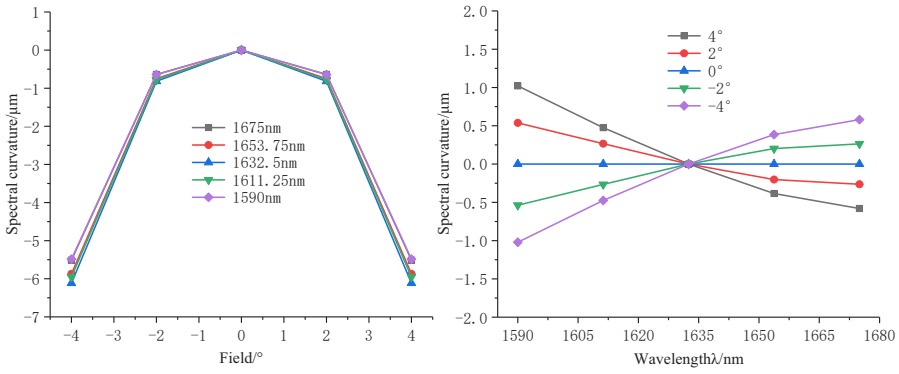

Fig. 10. The line of spectral smile and keystone.

Optics EXPRESS

As can be seen from Fig. 10, in the wavelength range of 1590-1675 nm, the spectral smile and keystone of the system are less than 6μm, and both are less than 1/3 of the combined pixel size. Data processing does not require correction.

The above optical design software simulation verifies the feasibility of the spectrometer design method proposed in this paper. This design method can not only achieve linear dispersion and compact structure, but also provide nanoscale spectral resolution. It also has low spectral line bending and color distortion, which further reduces the difficulty of subsequent image processing.

4. Analysis of influence

In order to verify that the method discussed in this paper has certain universality and analyze the influence factors of dispersion nonlinearity. This method is used to design a small F-number hyperspectral imager with different indexes. The working band is 1050-1600 nm and the spectral resolution is 1.2 nm. The design results show that the system $|K_m - 1|<0.0011$ also has good dispersion uniformity.

4.1. Material

Based on the above design, we keep the lens set parameters for collimation and focusing imaging unchanged, replace the material for the immersion grating dispersion module, and evaluate its dispersion nonlines with $K_m - 1$, as shown in Table 2.

Table 2. Structure parameter list

Number	Material 1	Material 2	α	β	$K_1 - 1$	$K_2 - 1$	$K_3 - 1$
1	HZK1	HZK1	29.87°	8.26°	0.01115	-0.00138	0.00208
2	NLAF34	SF11	-30.00°	8.11°	-0.00710	-0.00104	-0.00208
3	ZF6	HLAK10	15.04°	5.06°	0.00301	0.00047	0.00288
4	HZK1	HLAF51	29.87°	5.69°	-0.00093	-0.00376	-0.00042
5	ZF6	SILICA	14.06°	3.98°	-0.00101	-0.00029	-0.00019
6	SILICA	ZF6	-10.93°	3.77°	-0.00100	-0.00010	0.00065

According to the data analysis in Table 2, the greater the difference between the refractive index of material 1 and that of material 2, the better the uniform dispersion ability. At the same time, the deflection angle α between the two materials has a certain relationship with the refractive index of the material. When the refractive index difference of the two materials is large, the deflection angle α is smaller than that of the two materials with similar refractive index, and the corresponding dispersion module size is smaller.

4.2. Structural parameter

Because of the different dispersion characteristics of different materials, it is impossible to simply compare the trend of dispersion nonlinearity with the change of two deflection angles. Therefore, the material is the same dispersion module, using the control variable method, to compare the influence of two deflection angles on dispersion uniformity. In Fig. 11, the horizontal coordinate is the deflection angle of the variable, and the vertical coordinate is the value of the dispersion uniformity evaluation index $K_m - 1$.

It can be seen that the deflection angle α between the two materials and the deflection angle β of the grating surface have a great influence on the dispersion uniformity of the system. Among them, the three curves corresponding to the deflection angle β are farther away from the zero value of the ordinate, and the influence is relatively greater. The three curves corresponding to the deflection angle α all pass the zero value of the ordinate. It can be seen that with the increase of the deflection angle α, the dispersion is gradually uniform until it is adjusted to the limit that

Optics EXPRESS

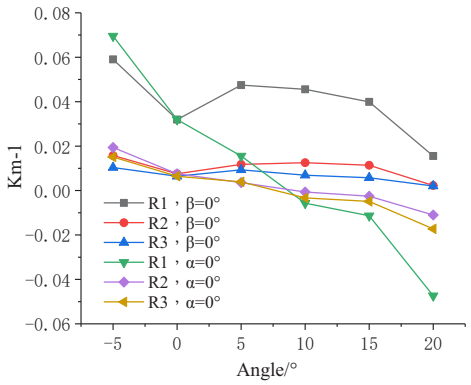

Fig. 11. Influence of deflection angle on dispersion.

the structure can reach. With the continuous increase of the deflection angle α, the dispersion begins to be uneven in the opposite direction.

4.3. Grating: Diffraction order and linear density

Both the diffraction order and the linear density of the grating have a great influence on the dispersion uniformity, and are inversely proportional to the dispersion uniformity. In other words, the stronger the dispersion ability of the grating, the greater the dispersion nonlinearity. Through the above two sections of analysis, it is possible to adjust the two materials first, by increasing the refractive index difference between them, to leave enough room for subsequent angle adjustment. Then, by adjusting the deflection angle, the maximum dispersion nonlinear correction is realized on the basis of ensuring the reasonable structure.

5. Conclusions

The immersion grating with high diffraction order can greatly reduce the volume and weight of the system while achieving high spectral resolution. However, immersion grating also brings more serious dispersion nonlinearity, which will cause some difficulties in the subsequent image processing and calibration. Therefore, we propose a design method of two material immersion grating to correct the spetral dispersion nonlinearity, and a short-wave infrared small F-number imaging spectrometer based on the proposed two-material immersion grating is designed. By deducing the initial structure of the spectral module, combining with the subsequent optimization, the obtained design can achieve better optical properties such as uniform dispersion, small F-number and high spectral resolution.

This method is applied to the actual imaging spectrometer design. The whole system is composed of telescope and spectrometer, which is designed via independent design and integrated optimization process. The design results show that in the band of 1590-1675 nm, the spectral resolution is better than 0.25 nm, the image square F-number is 2, $|K_m - 1|$<0.0018, much less than 0.003, and the dispersion uniformity is good. Spectral smile and keystone are less than 6μm, less than 1/3 of the combined pixel size. MTF is better than 0.83 when the cutoff frequency is 25lp/mm, the RMS radius is less than 7μm, and the image quality meets the requirements. The collimation system and the imaging system are the same set of lenses, which is easy to process and adjust, and further achieve a compact structure. The short-wave infrared small F-number imaging spectrometer based on two-material immersion grating as dispersion module can meet the practical application requirements. This paper can provide a certain degree of reference for researchers in related fields.

Optics EXPRESS

Funding. Earth-moon large dynamic range high precision imaging spectrum technology (2022YFB3903202); National Natural Science Foundation of China (62205330); Strategic Priority Research Program of the Chinese Academy of Sciences (XDA28050103).

Acknowledgments. Thanks for the fund support.

Disclosures. The authors declare no conflicts of interest.

Data availability. No data were generated or analyzed in the presented research.

References

1. C. E. Alissandrakis and J. C. Vial, "Explosive Events in the Quiet Sun Near and Beyond the Solar Limb Observed with the Interface Region Imaging Spectrograph (IRIS)," Sol. Phys. **298**(2), 18–22 (2023).
2. J. C. Zhu, Z. C. Zhao, Q. Liu, X. H. Chen, H. Li, S. F. Tang, and W. M. Shen, "Geostationary Full-Spectrum Wide-Swath High-Fidelity Imaging Spectrometer: Optical Design and Prototype Development," Remote Sens. Basel **15**(2), 396 (2023).
3. H. Liu, X. S. Hou, B. L. Hu, T. Yu, Z. F. Zhang, X. Liu, J. C. Liu, X. J. Wang, J. J. Zhong, and Z. X. Tan, "Image blurring and spectral drift in imaging spectrometer system with an acousto-optic tunable filter and its application in UAV remote sensing," Int. J. Remote Sens. **43**(19-24), 6957–6978 (2022).
4. Q. G. Song, Y. Z. Dai, X. P. Xiao, Q. Z. Sun, K. M. Zhou, L. Zhang, and Z. J. Yan, "Diffraction characteristics of radiated tilted fiber grating and its spectrometer application," Opt. Express **30**(13), 22538–22549 (2022).
5. H. Brandon, M. Faraz, and F. Yeshaiahu, "Channel dispersed Fourier transform spectrometer," Commun. Phys. **1**(1), 34 (2018).
6. S. Wu, C. Huang, L. Yu, H. Xue, and J. Lin, "Optical design and evaluation of an advanced scanning Dyson imaging spectrometer for ocean color," Opt. Express **29**(22), 36616–36633 (2021).
7. D. M. Kita, B. Miranda, D. Favela, D. Bono, J. Michon, H. Lin, T. Gu, and J. J. Hu, "High-performance and scalable on-chip digital Fourier transform spectroscopy," Nat. Commun. **9**(1), 4405 (2018).
8. A. Thumm, M. Riddell, B. Nanayakkara, J. Harrington, and R. Meder, "Mapping Within-Stem Variation of Chemical Composition by near Infrared Hyperspectral Imaging," J. Near Infrared Spec. **24**(6), 605–616 (2016).
9. W. A. Traub, "Constant-dispersion grism spectrometer for channeled spectra," J. Opt. Soc. Am. A **7**(9), 1779–1791 (1990).
10. B. Jorge, M. Emmanuel, and A. Henry, "Computational spectral imaging: a contemporary overview," J. Opt. Soc. Am. A **40**(4), C115–C125 (2023).
11. J. W. Wang, W. Y. Li, J. Y. Sun, B. Li, X. W. Chen, Z. Tan, N. Zhao, Y. Y. Liu, and Q. B. Lu, "Fast Spectral Calibration Method of Spectral Imager," Spectrosc. Spect. Anal. **42**(07), 2013–2017 (2022).
12. L. Yin, J. Bayanheshig, Y. X. Yang, R. Lu, C. Zhang, J. C. Sun, and Cui, "High-accuracy spectral reduction algorithm for the échelle spectrometer," Appl. Opt. **55**(13), 3574–8 1 (2016).
13. M. Shen, Z. Q. Hao, X. Y. Li, C. M. Li, L. B. Guo, Y. Tang, P. Yang, X. Y. Zeng, and Y. F. Lu, "New spectral reduction algorithm for echelle spectrometer in laser-induced breakdown spectroscopy," Opt. Express **26**(26), 34131–34141 (2018).
14. J. Z. Fan, B. Li, X. Ye, H. S. Li, and G. Y. Lin, "Dyson Prism Imaging Spectrometer with Long Slit and Uniform Dispersion," Appl. Opt. **50**(35), 6487 (2011).
15. B. Liu, Y. Liu, X. L. Zhang, C. Li, J. Wang, C. Li, and Q. Sun, "Study on Coaxial Linear Dispersion Triplet Prisms of Wide Spectral Imaging Spectrometer," Spectrosc. Spect. Anal. **36**(05), 1543–1548 (2016).
16. C. Yoon, A. Bauer, D. Xu, C. Dorrer, and J. P. Rolland, "Absolute linear-in-k spectrometer designs enabled by freeform optics," Opt. Express **27**(24), 34593–34602 (2019).
17. T. Vaarala, M. Aikio, and H. Keraenen, "Advanced prism-grating-prism imaging spectrograph in online industrial applications," Proc. SPIE **3101**, 322–330 (1997).
18. X. Zhang, J. Wang, J. Zhang, J. Yan, and Y. Han, "A design method for direct vision coaxial linear dispersion spectrometers," Opt. Express **30**(21), 38266–38283 (2022).
19. R. X. Wang, M. A. Ansari, H. Ahmed, Y. Li, W. F. Cai, Y. J. Liu, S. T. Li, J. L. Liu, and X. Z. Chen, "Compact multi-foci metalens spectrometer," Light: Sci. Appl. **12**(1), 103 (2023).
20. J. Reimers, A. Bauer, K. P. Thompson, and J. P. Rolland, "Freeform spectrometer enabling increased compactness," Light: Sci. Appl. **6**(7), e17026 (2017).
21. X. H. Zhou, Y. H. Gong, S. H. Wu, Y. K. Wang, Y. F. Huang, H. W. Ye, G. W. Wang, and Y. C. Wang, "Derivation and application of expression methods based on law of reflection and refraction of light," J. Appl. Opt. **43**(3), 510–517 (2022).
22. P. Xesús, G. Héctor, and F. L. D. Raúl, "Off-plane anastigmatic imaging in Offner spectrometers," J. Opt. Soc. Am. A **28**(11), 2332–2339 (2011).
23. X. D. Bayanheshig, Y. G. Qi, and Tang, "The vector diffraction theory analysis of chromatic dispersion characteristics of phase grating," Acta Phys. Sin. **52**(5), 1157–1161 (2003).
24. G. Thuillier, P. Zhu, M. Snow, P. Zhang, and X. Ye, "Characteristics of solar-irradiance spectra from measurements, modeling, and theoretical approach," Light: Sci. Appl. **11**(1), 79 (2022).
25. X. Ye, X. L. Yi, C. Lin, W. Fang, K. Wang, Z. W. Xia, Z. H. Ji, Y. Q. Zheng, D. Sun, and J. Quan, "Instrument Development: Chinese Radiometric Benchmark of Reflected Solar Band Based on Space Cryogenic Absolute Radiometer," Remote Sens. Basel **12**(17), 2856 (2020).